Theor Chem Acc (2002) 108:1–11
DOI 10.1007/s00214-002-0344-z

Theoretical
Chemistry Accounts

Feature article

Recent applications of density functional theory calculations to biomolecules

Fuqiang Ban[1], **Kathryn N. Rankin**[1], **James W. Gauld**[2], **Russell J. Boyd**[1]

[1] Department of Chemistry, Dalhousie University, Halifax, Nova Scotia B3H 4J3, Canada
[2] Department of Chemistry and Biochemistry, University of Windsor, Windsor, Ontario N9B 3P4, Canada

Received: 19 December 2001 / Accepted: 8 April 2002 / Published online: 4 July 2002

Abstract. The purpose of this overview is to highlight the broad scope and utility of current applications of density functional theory (DFT) methods for the study of the properties and reactions of biomolecules. This is illustrated using examples selected from research carried out within our research group and in collaboration with others. The examples include the hyperfine coupling constants of amino acid radicals, the use of an amino acid as a chiral catalyst for the formation of carbon–carbon bonds in the aldol reaction, hydrogen-bond mediated catalysis of an aminolysis reaction, radiation-induced protein–DNA cross-links, and the mechanism by which an antitumor drug cleaves DNA. We demonstrate that DFT-based methods can be applied successfully to a broad range of problems that remain beyond the scope of conventional electron-correlation methods. Furthermore, we show that contemporary computational quantum chemistry complements experiment in the study of biological systems.

Key words: Density functional theory – Biological molecules – Hyperfine coupling constants – Amino acid radicals – Aldol reaction

1 Introduction

There has long been interest in understanding the properties and functions of important biochemical species ranging from small biological signaling agents to enzymes. Recently, there have been rapid improvements in our ability to identify, isolate and characterize biological molecules. This has been perhaps most dramatically highlighted by the rapidity by which the first draft of the human genome was obtained. However, despite these developments there remain many biochemical problems that are very difficult or impossible to investigate experimentally owing to short lifetimes and/or high reactivity of the relevant species. Examples include the characterization of the intermediates of enzymatic mechanisms.

Recently, the scope of the application of computational chemistry has undergone great expansion owing to the advent of more powerful computers and the development of new theoretical methods and algorithms [1]. In particular, developments in density functional theory (DFT) have provided alternatives to more conventional electron correlation methods, for example, MP2 and QCISD. Numerous studies [1, 2] have demonstrated the reliability and accuracy of DFT methods for a range of chemical properties and reactions. Blomberg and Siegbahn [3] have reviewed their mechanistic study of redox-active metal enzymes using model systems with more than 50 atoms at the B3LYP level of theory. Furthermore, the noticeable computational efficiency and accuracy of well-behaved density functional methods, such as B3LYP, has prompted the development of many promising procedures for a full exploration of the chemistry of enzymatic systems at more realistic scales than ever before. Using a hybrid computational scheme of DFT and molecular mechanics, Cui and coworkers and Dinner et al. [4] have reported mechanistic studies of several enzymes, including the liver alcohol dehydrogenase, triosephosphate isomease and uracil–DNA glycosylase. By the use of a hybrid computational scheme of DFT methods and lower levels of theory in the ONIOM methodology, Torrent and coworkers [5] have demonstrated that very large biological systems, such as the methane monooxygenase and the ribonucleotide reductase, can be modeled to high accuracy. The application of DFT methods in Car–Parrinello molecular dynamic simulations has been reviewed recently by Carloni and Rothlisberger [6]. Thus, the potential for computational investigations using DFT methods to complement or guide experiments on biomolecules and enzymatic mechanisms is clearly established.

A comprehensive review of recent applications of DFT calculations to biomolecules and biochemical problems is beyond the scope of this short review. Instead, the purpose of this review is to illustrate and

Correspondence to: R.J. Boyd
e-mail: russell.boyd@dal.ca

provide an overview of some current applications of DFT methods to the study of the properties and reactions of biomolecules. This is done using examples from our research group and from collaborations undertaken with others, which range from the calculation of hyperfine coupling constants (HFCCs) of amino acid derived radicals to the catalytic potential of nucleobases and the mechanism of action of an antitumor drug. For a more detailed discussion of each application of DFT, the reader is referred to the appropriate literature.

For the topics included in this overview, all the geometry optimizations were performed using the GAUSSIAN 98 suite of programs [7] and were obtained using the B3LYP functional [8, 9]. Harmonic vibrational frequencies and zero-point vibrational energies were obtained at the same level of theory as used for the geometry optimizations. Relative energies were calculated by performing B3LYP single-point energy calculations with larger basis sets. HFCCs were calculated using the deMon [10] program and the PWP86 functional [11]. All relative energies are in kilojoules per mole.

2 Structures and HFCCs of amino acid radicals: hydroxyproline

Protein-derived radicals [12] are important intermediates not only for enzymatic catalysis [13] but also for oxidative damage to proteins [14, 15]. In order to understand complex questions arising from sophisticated protein-derived radicals, amino acid derived radicals are often utilized as model systems [14, 16, 17]. Electron spin resonance (ESR) and related techniques are powerful tools for investigating radical species [18]. For amino acid radicals, the protons are by far the most common and most important magnetic nuclei for detection; however, it is often extremely difficult to separate all hyperfine coupling tensors of the protons in a complex ESR spectrum. For example, the HFCCs of the protons of the carboxylic group of amino acids are often too small to be detected [19, 20, 21]. Thus, theory may provide complementary information to experiments for the characterization of unknown radical species.

Accurate prediction of HFCCs requires theoretical methods that provide a high level of electron correlation recovery [22]. Highly accurate conventional electron correlation methods [23] are generally too expensive to investigate the HFCCs of biological radicals. However, DFT methods offer a computationally cheaper but quite accurate alternative and, at present, are the preferred choice for calculating the HFCCs of biological radicals [24].

In view of the success of our comprehensive studies of radicals formed from the components of DNA [25], and the resultant multicomponent model for radiation damage to DNA from its constituents [26], we have used a similar approach for the investigation of amino acid radicals. Our systematic calculations on glycine- [27], alanine- [28], and hydroxyproline-derived [29] radicals indicate that the PWP86/6-311G(2d,p)//B3LYP/6-31 + G(d,p) calculations on the gas-phase structures of those isolated amino acid radicals shown in Fig. 1 reproduce the observed proton HFCCs in the single crystals. Amino acids exist as zwitterionic species in the crystalline state and in solution; however, it has been shown that the zwitterionic structures of amino acids and their derived radicals do not correspond to energy minima in the gas-phase [30, 31]. Thus, in order to obtain the zwitterionic structures of amino acids and their radicals, the environmental effects have to be taken into account. Rega et al. [31] demonstrated that the zwitterionic structure of the glycine R1 radical can be obtained using B3LYP/6-31 + G(d,p) together with the conductor-like polarizable continuum model, and we showed that zwitterionic structures of glycine, alanine, and hydroxyproline radicals can be effectively obtained using B3LYP/6-31 + G(d,p) together with the Onsager model. The gas-phase PWP86/6-311G(2d,p) calculations on the zwitterionic structures of the radicals in Fig. 2, provide HFCCs in good agreement with the experimental data obtained for single crystals.

The HFCCs of an amino acid radical depend on its protonation state and conformation; thus, DFT HFCC calculations on the possible conformers of all related forms of a proposed radical may lead to a more accurate assignment of the observed HFCCs and provide deeper insight into the correlation between structure and the observed HFCCs. For example, upon irradiation of hydroxyproline the two observed H_β hyperfine tensors (the isotropic HFCCs, A_{iso}, are 23.9 and 61.0 MHz) were assigned to two different conformations of the zwitterionic radical R^Z (Fig. 3) as no carboxylate hydrogen interactions were detected [32]. However, our calculations suggested that the assignment is inaccurate. Because proton transfer may be involved in the formation of a radical in an irradiated hydroxyproline single crystal, we systematically examined the zwitterionic

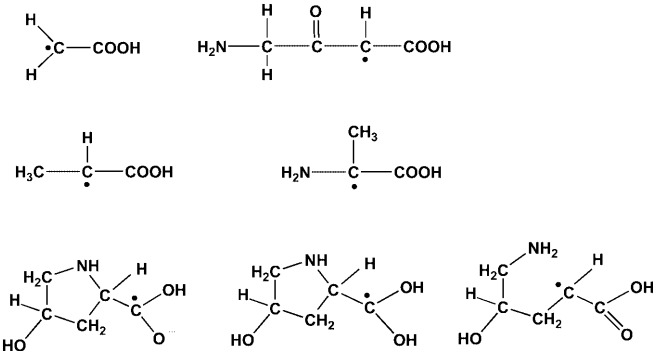

Fig. 1. Schematic illustration of the structures of the nonzwitterionic radicals of glycine, alanine, and hydroxyproline

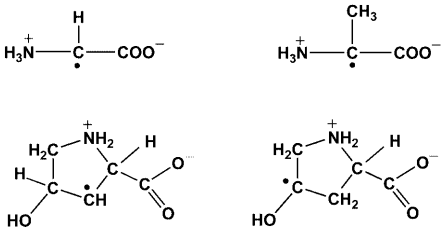

Fig. 2. Schematic illustration of the structures of the zwitterionic radicals of glycine, alanine, and hydroxyproline

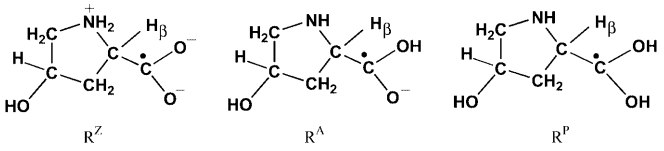

Fig. 3. Schematic illustration of the structures of R^Z, R^A, and R^P

radical anion R^Z, its nonzwitterionic radical anion R^A and the protonated neutral radical R^P (Fig. 3) [29]. Two possible conformers of R^Z, four conformers of R^A, and four conformers of R^P were obtained by a conformational search at the B3LYP/6-31 + G(d,p) level.

The PWP86/6-311G(2d,p) calculated H_β A_{iso} of R^Z, R^A, and R^P are significantly different in magnitude. The calculated H_β isotropic HFCCs of R^Z are smaller than 5 MHz, far different from either of the two observed A_{iso}. The calculated H_β isotropic HFCCs of two of the four conformers of R^A are approximately 20 MHz, while the calculated H_β isotropic HFCCs of the four conformers of R^P are approximately 60 MHz. Thus, the DFT calculations clearly elucidated that the two observed hyperfine coupling tensors are in fact given by R^A and R^P and not, as previously proposed, by two conformations of R^Z.

3 Amino acids as chiral catalysts: the proline catalyzed aldol reaction

Nature's catalysts, enzymes, enable a myriad of chemical transformations to occur in biological systems [33]. The chiral nature of these enzymes results in the accelerated formation of reaction products with well-defined regio- and stereochemistry. As such, notable attention has been directed towards the development of antibody-based catalysts (or biocatalysts) [34, 35, 36]. These novel biocatalysts often catalyze chemical reactions by employing a mechanism analogous to that observed for the natural enzyme and do so with high efficiency and stereochemical control. Biocatalysts that accept a wide range of substrates, yielding products of high enantiopurity, are of particular interest to synthetic chemists [34, 36].

Recently, List et al. [37] found that the simple amino acid L-proline catalyzes the aldol reaction between acetone and a variety of aldehydes, yielding the desired aldol products in good yields and with high enantioselectivities. They proposed that, analogous to enzymatic conversions involving class 1 aldolases, proline may be used as a catalyst to enable the "direct" asymmetric aldol reaction to occur via an enamine mechanism (Fig. 4). As such, the ketone moiety is not required to undergo preconversion to its enol derivative, as has been historically required to achieve an asymmetric catalytic aldol reaction [38, 39].

The enamine mechanism proposed by List et al. [37] for the direct aldol reaction between acetone and a variety of aldehydes was examined using B3LYP/6-311 + G(2df,p)//B3LYP/6-31G(d,p) calculations on the model reaction of acetone with acetaldehyde in the presence of proline (Scheme 1). The effect of solvent on

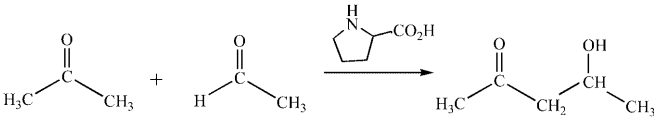

Scheme 1. Schematic illustration of the proline-catalyzed aldol reaction between acetone and acetaldehyde

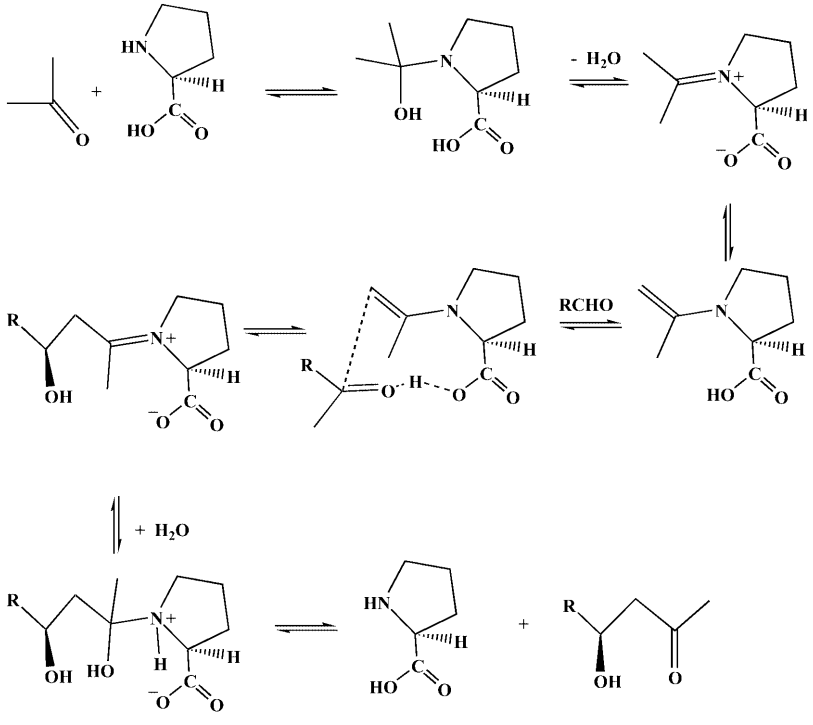

Fig. 4. Proposed enamine mechanism of the proline-catalyzed aldol reaction (from Ref. [31])

the enamine mechanism was investigated using the Onsager model. A dielectric constant of 46.7 was utilized to model the use of dimethyl sulfoxide (DMSO) as the solvent in the original reaction conditions [37].

There exists a close relation between the reaction mechanism of the class 1 aldolases [34, 35, 36] and the postulated mechanism of the proline catalyzed direct aldol reaction [37, 40]. The initial process in both mechanisms involves the formation of an enamine complex generated by the reaction of the ketone with the amino functional group of proline. This enamine undergoes tautomerism to yield the imine, which then reacts with the aldehyde to generate the aldol product. The gas-phase DFT calculations indicate that the initial interaction between proline and the ketone has a very large barrier that may inhibit further progression of the reaction (Fig. 5a). However, inclusion of the effects of a moderately ionizing solvent, for example, DMSO, results in a significantly lower-energy alternative pathway being found for the initial interaction between proline and acetone to form the enamine intermediate (Fig. 5b). Equivalent structural and energetic trends for the remainder of the mechanism outlined in Fig. 4 are reproduced by the DFT calculations in the gas phase and in the presence of DMSO. Thus, the use of DFT methods enables one to obtain greater insight into the mechanism by which the amino acid proline catalyzes the direct aldol reaction between acetone and acetaldehyde [41] and reveals the important role the solvent plays in the aldol reaction.

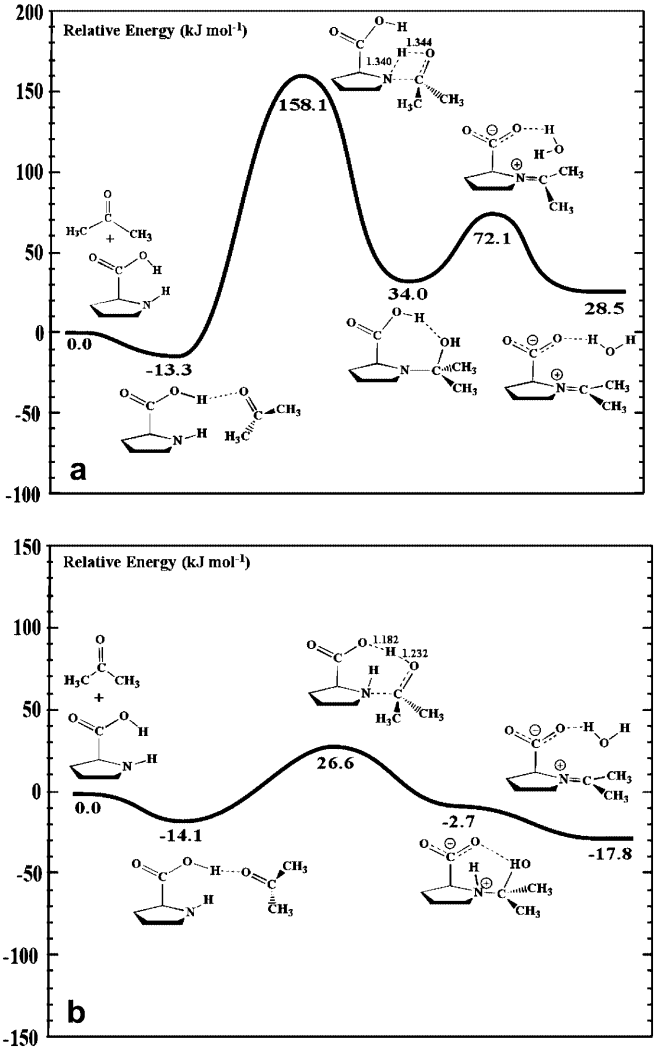

Fig. 5. Schematic illustration of the initial interaction between proline and acetone in **a** the gas phase and **b** the presence of dimethyl sulfoxide

4 Hydrogen-bond-mediated catalysis: aminolysis of 6-chloropyrimidine

Many enzymes accelerate chemical reactions in biological systems by selectively binding and stabilizing the transition structure [42]. The formation of multiple hydrogen bonds facilitates rapid molecular recognition and subsequent chemical reactions [43]. As a result, molecules capable of forming hydrogen bonds have been employed as catalysts in reactions of organic and biological importance [44, 45].

Recently, Tominaga et al. [46] reported that derivatives of the nucleobase uracil catalyze the aminolysis of 6-chloropurine and related species. On the basis of ^{1}H NMR, this catalytic behavior was proposed to occur as a result of the formation of multiple hydrogen-bonding interactions between the uracils and 6-chloropurine derivatives via a reactive intermediate and a stabilized transition structure (Fig. 6). To provide a rationalization for the role of the hydrogen-bonding interactions, B3LYP/6-311 + G(2df,p)//B3LYP/6-31G (d,p) calculations were performed on the model reaction: aminolysis of 6-chloropyrimidine (Scheme 2a) [47].

In the "isolated" system (Fig. 7a), i.e., aminolysis of 6-chloropyrimidine with no additional hydrogen-bonding bases included, the reaction proceeds with a barrier of approximately 138 kJ mol^{-1}. On the basis of the hydrogen-bonding motif of uracil, the effect of adding H_2CO or H_2NCHO was considered. The addition of the electron-donating species H_2CO (Fig. 7b) to NH_3 + $Cl{-}C_4N_2H_3$, enables the aminolysis of $Cl{-}C_4N_2H_3$ to proceed with a barrier that is about 26 kJ mol^{-1} lower than that of the isolated system. As H_2CO interacts with NH_3 via an O···H–N hydrogen bond in the transition structure, the electron-donating ability of the nitrogen of the NH_3 moiety is enhanced, thus enabling the transition

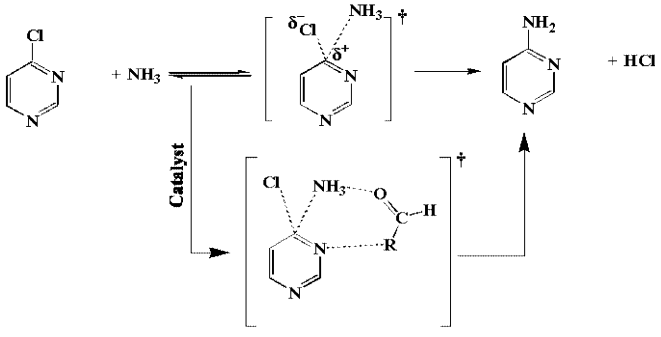

Fig. 6. Schematic illustration of the catalytic pathway for the aminolysis of 6-chloropyrimidine

structure for aminolysis to occur earlier. The aminolysis of NH_3 + Cl–$C_4N_2H_3$ involving the H_2NCHO moiety (Fig. 7c), which contains both electron-donating (–CHO) and electron-accepting ($-NH_2$) groups, proceeds with a barrier about 43 kJ mol^{-1} lower than the isolated aminolysis. In the transition structure for this aminolysis, H_2NCHO is hydrogen bonded to both the incoming NH_3 moiety and to the nitrogen of the pyrimidine ring. Thus, as the electron-donating ability of the nitrogen of the incoming NH_3 moiety is enhanced by the electron-donating –CHO group, the negative charge of the nitrogen in the pyrimidine ring that is adjacent to the carbon at which substitution is occurring is simultaneously stabilized by the electron-accepting $-NH_2$ group, thereby facilitating an overall lowering in the barrier to aminolysis.

Hence, the catalytic potential of hydrogen-bonding moieties such as H_2CO and H_2NCHO is illustrated by the DFT study of the aminolysis of 6-chloropyrimidine [47]. A subsequent DFT study [48] of the effect of larger hydrogen-bonding moieties such as OCHNHHCO and 1-methyluracil on the aminolysis of 6-chloropyrimidine (Scheme 2a) and its 2-amino derivative (Scheme 2b), further revealed a correlation between the proton affinity of the carbonyl group of the hydrogen-bonded moiety interacting with the incoming NH_3 and the barrier to aminolysis. Specifically, as the proton affinity of the carbonyl group increases, the barrier to aminolysis decreases. These DFT studies [47, 48] of the aminolysis of 6-chloropyrimidine and 2-amino-6-chloropyrimidine elegantly illustrate the ability of the functional groups in uracil to catalyze the reaction by formation of multiple hydrogen bonds.

5 Radiation-induced protein-DNA cross-linking

The importance of radical chemistry in living systems has been increasingly appreciated by biologists and chemists [15]. Large quantities of common reactive-oxygen species (ROS), such as the hydroxyl radical, can be generated from endogeneous cellular metabolism and external perturbations (such as ionizing radiation) [14, 15]. The attack of ROS on DNA and proteins produces

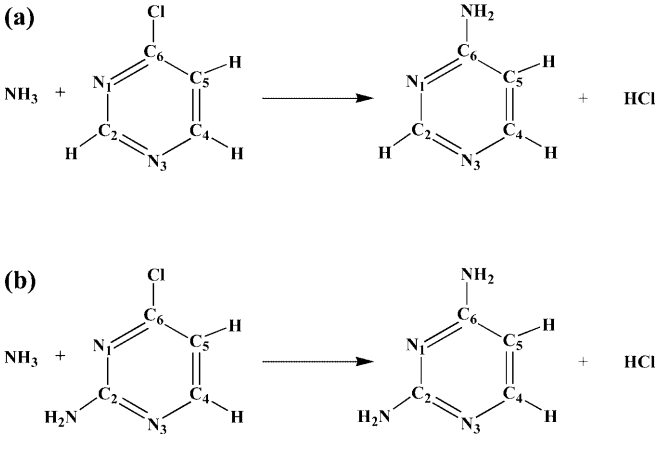

Scheme 2. Schematic illustration of the aminolysis of **a** 6-chloropyrimidine and **b** 2-amino-6-chloropyrimidine

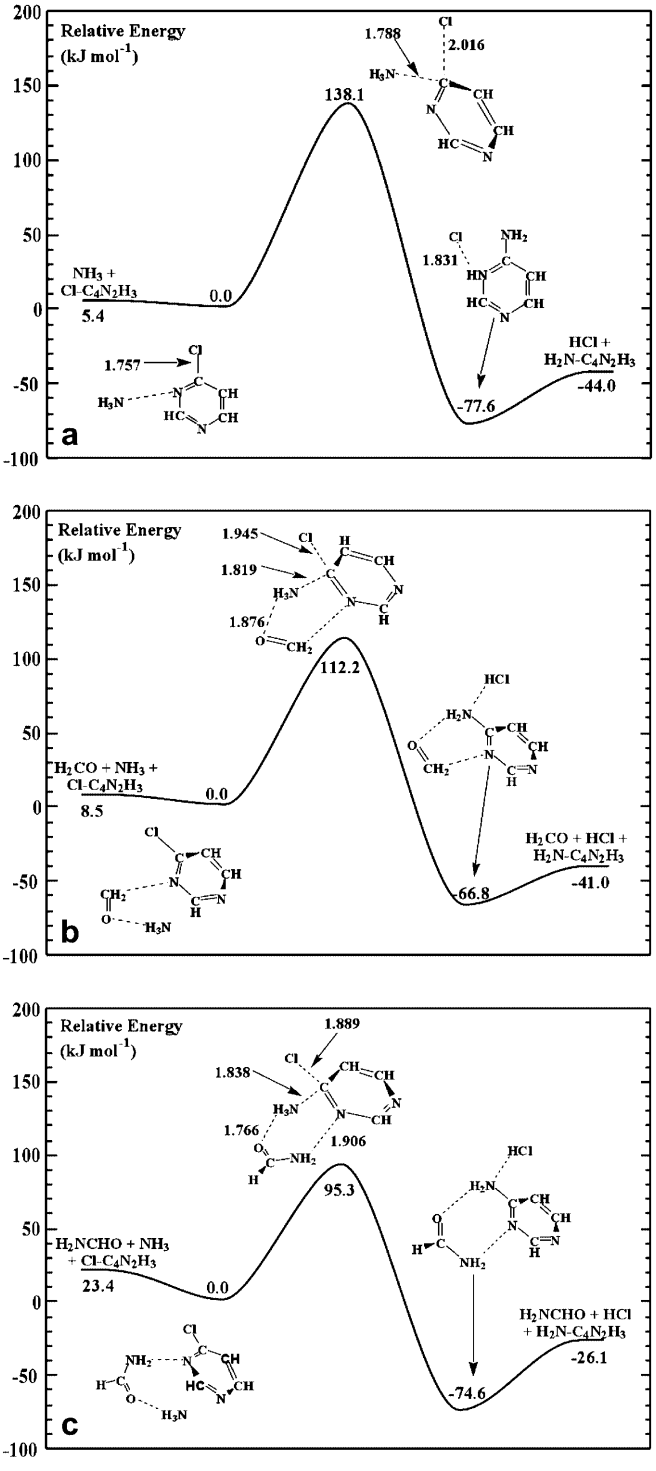

Fig. 7. Schematic energy profiles of aminolysis of 6-chloropyrimidine for **a** the "isolated" system, **b** with H_2CO hydrogen bonded to the NH_3 moiety and, **c** with H_2NCHO hydrogen bonded to the NH_3 moiety

radicals that ultimately lead to a diversity of modifications of DNA and proteins, and thereby cause numerous diseases [15, 49, 50, 51, 52, 53, 54, 55, 56].

It has been shown that ionizing radiation produces DNA–protein cross-links in living cells and isolated chromatin [57, 58, 59] by reaction with the hydroxyl

radical. Gajewski and Dizdaroglu [60] reported that a DNA–protein cross-link of cytosine and tyrosine moieties forms in a nucleohistone when exposed to γ-ray radiation. The cross-link was proposed to involve formation of a covalent bond between C_6 of cytosine and C_3 of tyrosine (the numbering of the atoms of cytosine and tyrosine is shown in Scheme 3). The cross-linking mechanisms were proposed [60] as shown schematically in Scheme 4: (1) the combination of cytosine C_5-hydroxylated radical and tyrosyl radical; (2) the addition of cytosine C_5-hydroxylated radical to tyrosine; (3) the addition of the tyrosyl radical to C_5 of cytosine; and (4) the addition of the tyrosyl radical to C_6 of cytosine. The last two mechanisms were suggested to be the addition of the tyrosyl radical to the C_5C_6 double bond of cytosine [60]. Moreover, it has been shown [60] that the cytosine–tyrosine cross-link in the nucleohistone is identical to the cross-link observed in the model experiments of the γ-ray irradiated aqueous solution of cytosine and tyrosine. Although only the radical combination mechanism was suggested to account for the formation of the cross-link in the aqueous vitro system, the radical addition mechanisms have not been eliminated.

In each of the mechanisms shown in Scheme 4, the final cross-link is formed through several steps of the reaction. As such, it is very important to examine the feasibility of every step of the reaction in each mechanism. In order to provide greater insight into the chemistry of the related cross-linking reactions, systematic calculations on the mechanisms at the B3LYP/6-311G(2df,p)//B3LYP/6-31G(d, p) level of theory using free cytosine and tyrosine (phenol) as model systems have been performed [61].

The initial cross-linking steps for the majority of the radical addition mechanisms considered were found to be thermodynamically unfavorable: they have a significant barrier to the formation of the initial cross-linked product (not shown). The only favored complete mechanism is initiated by a combination between the cytosine C_6 and the tyrosine C_3 to form the initial cross-linked product, which lies significantly lower in energy (-157.0 kJ mol^{-1}), Fig. 8a. This is then followed by a hydrogen shuffle (Fig. 8b): the cytosine moiety transfers a hydrogen to the tyrosine oxygen while simultaneously abstracting a

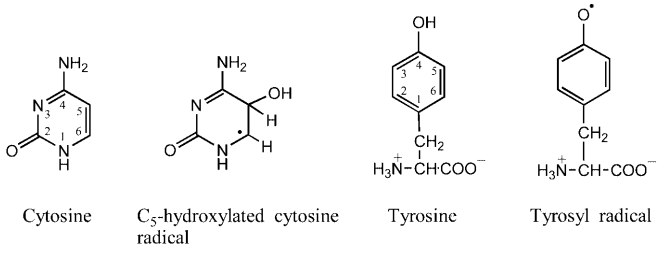

Scheme 3. Schematic illustration of the structures of cytosine, cytosine C_5 hydroxylated radical, tyrosine, and tyrosyl radical

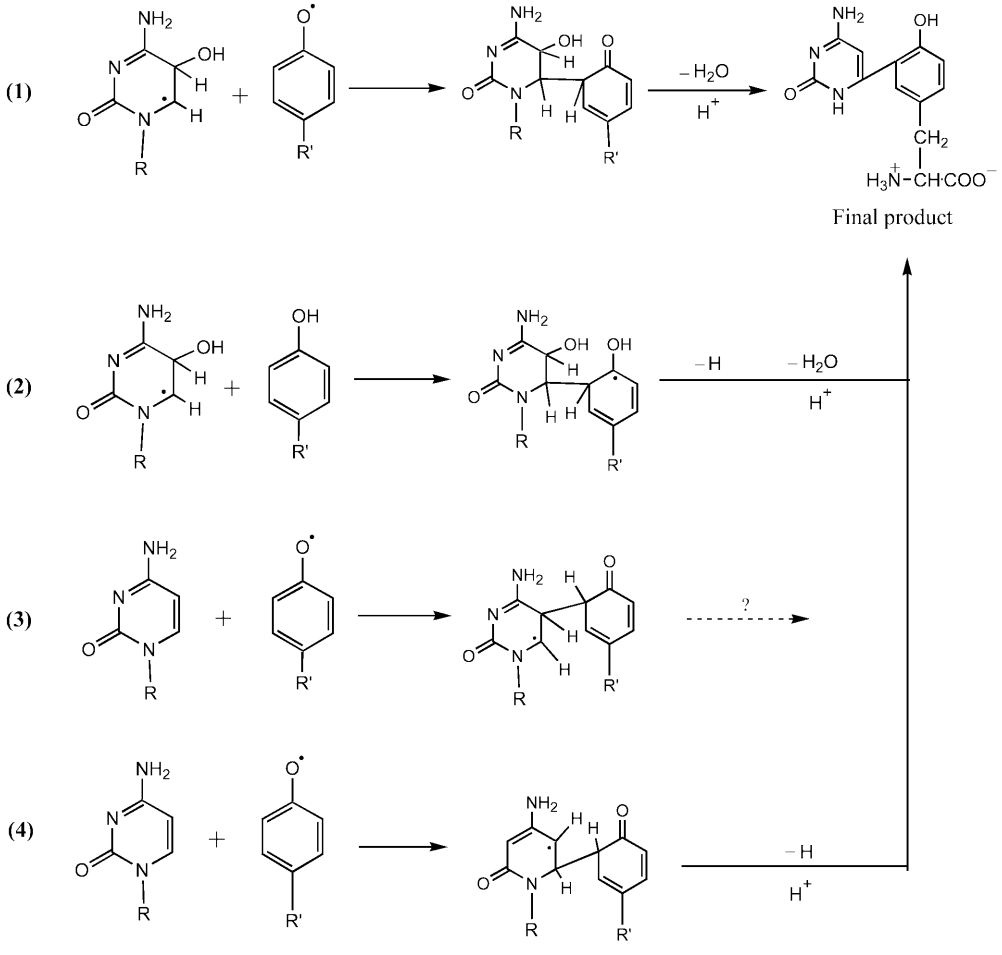

Scheme 4. Schematic illustration of the four cross-linking mechanisms investigated

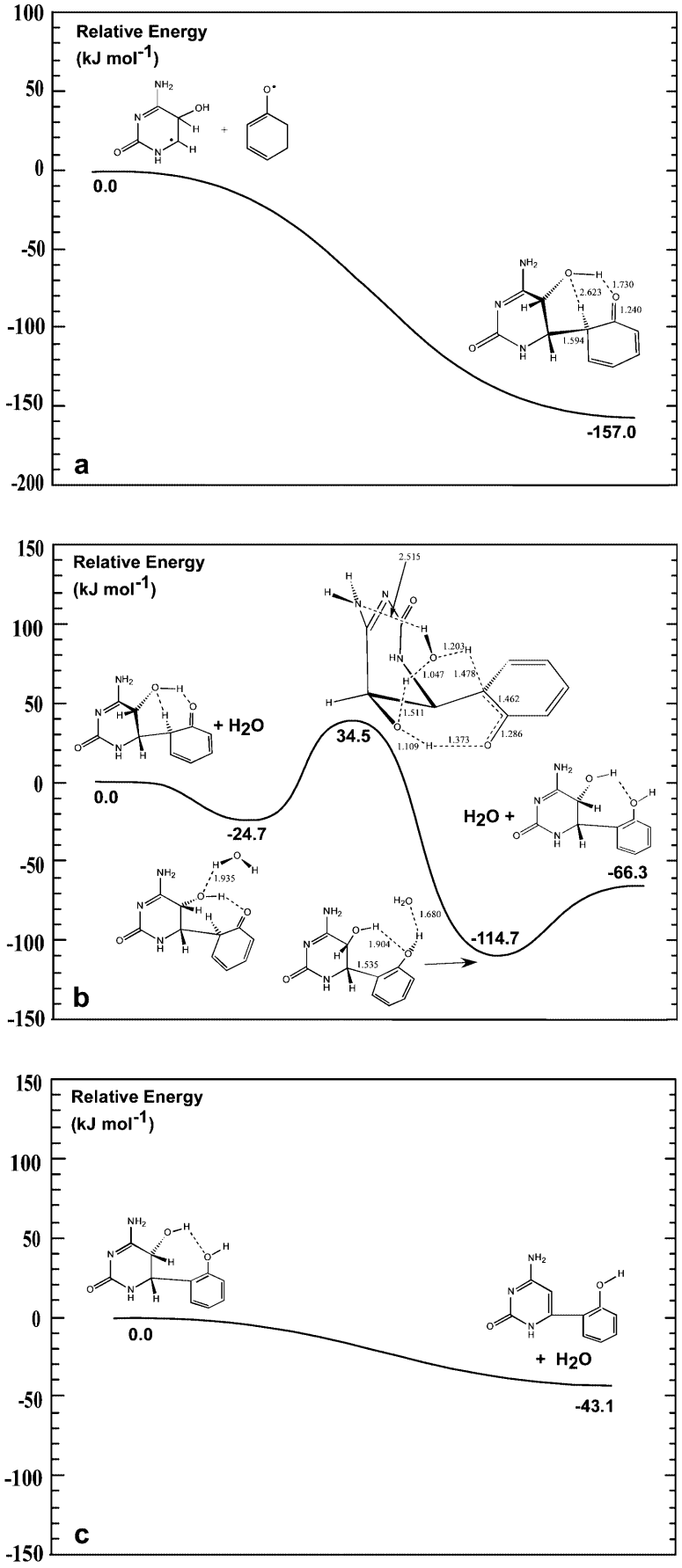

Fig. 8. Schematic energy profiles of the favored complete mechanism: **a** radical combination, **b** H_2O and hydrogen-bond-assisted hydrogen transfer, and **c** dehydration

hydrogen from a water molecule, which concomitantly abstracts the hydrogen from the cross-linked carbon site of the tyrosine! Hydrogen bonds play a key role in this hydrogen-transfer step. The final product is then formed by an acid-catalyzed dehydration reaction (Fig. 8c). In this study, DFT calculations elucidated a complete multiple-step mechanism by which protein–DNA cross-linking may occur. The fundamental effects of hydrogen bonds and a water molecule on the hydrogen transfer have been clearly demonstrated.

6 Action of the antitumor drug tirapazamine

Many cancerous tumors are oxygen-poor or hypoxic [62, 63, 64], and often quite resistant to more conventional forms of antitumor treatment such as radiotherapy and chemotherapy [55]. Consequently, there has been considerable effort to identify potential antitumor drugs that specifically target such cells. One such class of potential hypoxia-specific drugs is the benzotriazine di-*N*-oxides, of which a particularly promising candidate is 3-amino-1,2,4-benzotriazine-1,4-dioxide [66, 67, 68], or tirapazamine (Scheme 5).

Extensive experimental investigations [69, 70, 71, 72] have shown that tirapazamine derives its biological activity from its ability to cause DNA cleavage in hypoxic tumor cells. It is known that in vivo, under hypoxic conditions, tirapazamine may undergo an enzymatic one-electron reduction to form the activated intermediate **2**, which may decompose to **3**, releasing a hydroxyl radical (Scheme 5). Both **2** and the hydroxyl radical have been suggested [68, 72] to react with DNA to yield a sugar-C_1' radical which then reacts further to give the corresponding deoxyribonolactone (Scheme 6), a key intermediate leading to cleavage of the DNA. However, radical-mediated DNA cleavage depends on molecular oxygen [73]; thus, the involvement of **2** and $^{\bullet}OH$ does not explain the remarkable selectivity of tirapazamine towards hypoxic tumor cells.

It has been proposed [69, 71] that tirapazamine may act as a molecular oxygen surrogate or mimic in radical-mediated DNA damage reactions. In particular, a sys-

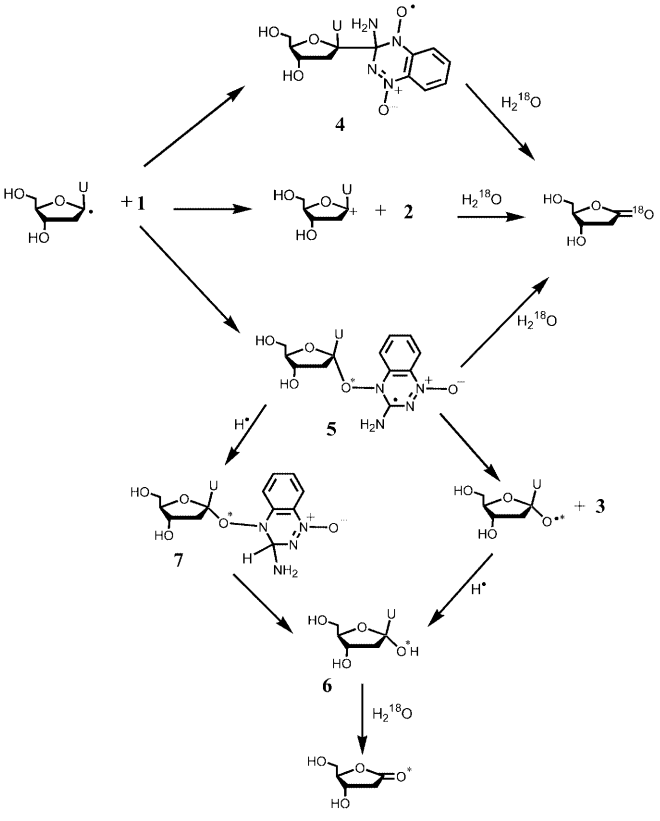

Scheme 7. Schematic illustration of the experimentally proposed mechanisms for the reaction of the sugar-C_1' radical with tirapazamine

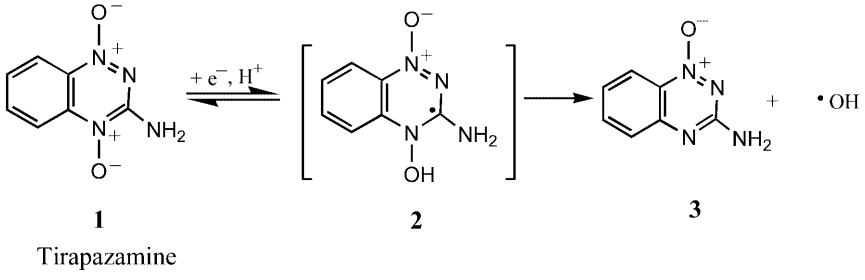

Scheme 5. Schematic illustration of the activation of tirapazamine by one-electron enzymatic reduction

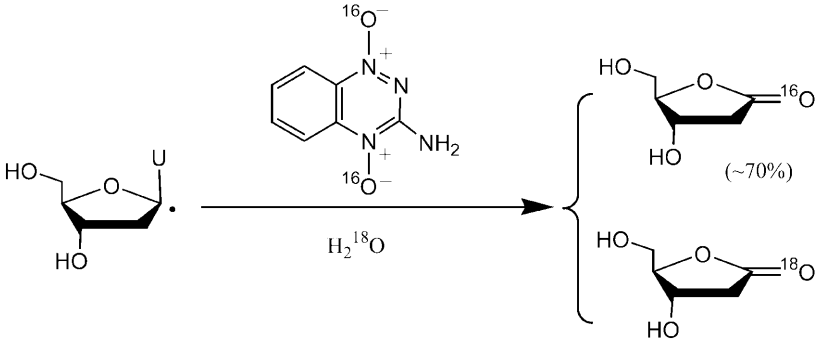

Scheme 6. Schematic illustration of the product distribution for the reaction of tirapazamine with a sugar-C_1' DNA radical

tematic experimental study of the reaction of tirapazamine with sugar-C_1' DNA radicals elucidated that the final deoxyribonolactone is formed predominantly through direct transfer of an *N*-oxide oxygen of the tirapazamine moiety to the sugar-C_1' radical. Only a minor amount was derived from direct attack of H_2O at the sugar-C_1' position (Scheme 6).

Hwang et al. [71] proposed that the direct oxygen transfer proceeds through the formation of the sugar–drug covalent adduct intermediate **5**, which may then react further by two possible mechanisms (Scheme 7). In one mechanism, the cross-linked N–O bond of intermediate **5** cleaves to produce an alkoxyl radical. Subsequent reduction of the alkoxyl radical forms the sugar-derived species **6** which can then hydrolyze to produce the corresponding deoxyribonolactone. In the alternative mechanism, an initial reduction of **5** occurs to give the neutral intermediate **7**. The cross-linked N–O bond then breaks, and hydrogen transfer to the oxygen of the now cleaved N–O bond gives the sugar-derived species **6** which, as already described, can then react further to give deoxyribonolactone. However, experiments do not differentiate between the two proposed reaction mechanisms.

In order to provide more insight into the chemistry of tirapazamine, we have performed systematic studies [74] on the mechanisms at the B3LYP/6-311G(d,p)//B3LYP/6-31G(d) level of theory using 1,2,4-triazaine dioxide and sugar radical model systems. The results clearly showed that the major steps in the cleavage of DNA strands by tirapazamine are the downhill reaction of the attachment of the oxygen end of tirapazamine to the sugar radical (see the calculated potential-energy surface in Fig. 9a) and the subsequent cleavage of the O–N bond of the tirapazamine moiety of the covalent adduct intermediate (see the calculated potential-energy surface in Fig. 9b) producing the alkoxyl radical. Further reactions of the alkoxyl radical can lead to the deoxyribonolactone, with concomitant cleavage of the DNA backbone.

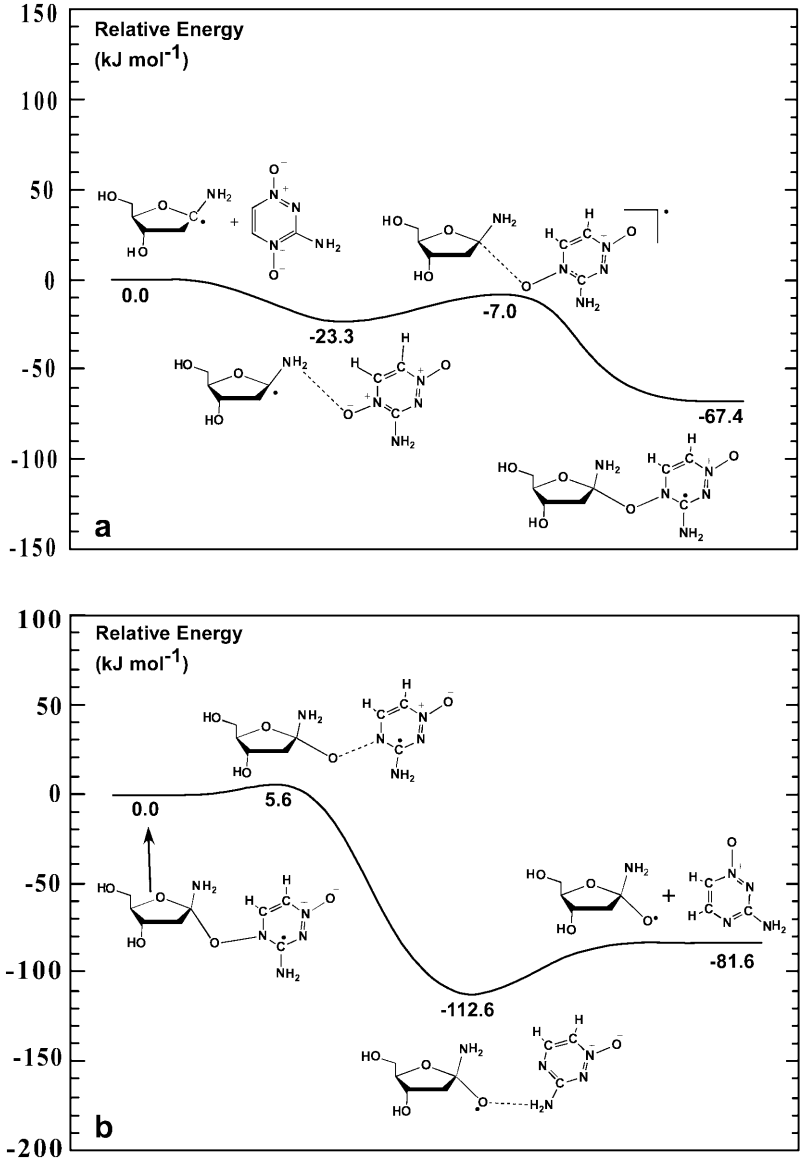

Fig. 9. Schematic energy profiles for **a** the formation of the carbon–oxygen covalent adduct intermediate and **b** the cleavage the O–N of the covalent adduct intermediate

7 Summary

One of the recurrent themes of our research is the use of computational quantum chemistry as a complementary tool for the investigation of systems that are not easily investigated by experimental techniques. By means of a few examples from our recent research, we have attempted to show that owing to recent advances in electronic structure theory, many properties of small molecules and radicals of biological interest can be predicted with sufficient accuracy to complement the results of experimental methods. Contemporary DFT-based methods are especially useful for the study of biological systems for which there is often little information on the identity of the principal biochemical species. We have also attempted to show how DFT-based methods can be used to elucidate reaction mechanisms by which biomolecules and drugs may affect the physiology of living systems. Such computational studies can provide valuable insight into enzyme catalysis and may prove useful for the design of catalysts for organic syntheses, including asymmetric synthesis. Finally, we note that such studies can be used to gain insight into the therapeutic importance of relatively small molecules [75].

Given that DFT-based methods can be successfully applied to a broad range of problems that remain beyond the scope of conventional electron-correlation methods, we believe that we are experiencing the dawn of a new era in computational quantum chemistry. High-level electronic structure calculations have only recently been employed to study biological systems at a realistic scale. The best applications have been for the prediction of molecular properties, such as HFCCs. Modeling the configurations of chemical (biological) systems with inclusion of the effects of the environment from hydrogen bonding, van der Waals, and steric interactions remains a great challenge to theoretical studies. However, an increasing amount of work on realistic biological systems at the DFT level of theory has appeared in the literature. In particular, the hybrid computational schemes of the quantum mechanics/molecular mechanics and the ONIOM methodologies are very promising for the explicit inclusion of the environment [4, 5, 76, 77]. The scope and application of DFT methods will increase with further development of efficient algorithms and more powerful computers, and with the continuing development of better computational strategies. The outlook for the future is, indeed, very bright.

Acknowledgements. We gratefully acknowledge the Natural Sciences and Engineering Research Council of Canada and the Killam Trusts for financial support. In addition, we also thank Leif A. Eriksson, Stacey D. Wetmore, and Maria Lundqvist for fruitful discussions and collaborations. K.N.R. thanks the Walter C. Sumner Foundation for a scholarship.

References

1. Friesner RA, Dunietz BD (2001) Acc Chem Res 34: 351
2. (a) Barone V (1995) Theor Chim Acta 91: 113; (b) Bauschlicher CW (1995) Chem Phys Lett 246: 40; (c) Chandra AK, Goursot A (1996) J Phys Chem 100: 11596; (d) Martell JM, Goddard JD, Eriksson LA (1997) J Phys Chem A 101: 1927; (e) Curtiss LA, Raghavachari K, Redfern PC, Pople JA (1997) J Chem Phys 106: 1063; (f) Lynch BJ, Truhlar DG (2001) J Phys Chem A 105: 2936
3. (a) Blomberg MRA, Siegbahn PEM (2001) J Phys Chem B 105: 9375; (b) Siegbahn PEM, Blomberg MRA (2000) Chem Rev 100: 421
4. (a) Cui Q, Karplus M (2002) J Phys Chem B 106: 1768; (b) Cui Q, Elstner M, Karplus M (2002) J Phys Chem B 106: 2721; (c) Cui Q, Karplus M (2001) J Am Chem Soc 123: 2284; (d) Dinner AR, Blackburn GM, Karplus M (2001) Nature 413: 752
5. (a) Torrent M, Vreven T, Musaev DG, Morokuma K, Farkas O, Schlegel HB (2002) J Am Chem Soc 124: 192; (b) Torrent M, Musaev DG, Basch H, Morokuma K (2001) J Comput Chem 23: 59
6. Carloni P, Rothlisberger U In: Eriksson LA (ed) (2001) Theoretical biochemistry, processes and Properties of biological systems. Elsevier, The Netherlands, p 215
7. Frisch MJ, Trucks GW, Schlegel HB, Scuseria GE, Robb MA, Cheeseman JR, Zakrzewski VG, Montgomery JA, Stratmann RE, Burant JC, Dapprich S, Millam JM, Daniels AD, Kudin KN, Strain MC, Farkas O, Tomasi J, Barone V, Cossi M, Cammi R, Mennucci B, Pomelli C, Adamo C, Clifford S, Ochterski J, Petersson GA, Ayala PY, Cui Q, Morokuma K, Malick DK, Rabuck AD, Raghavachari K, Foresman JB, Cioslowski J, Ortiz JV, Stefanov BB, Liu G, Liashenko A, Piskorz P, Komaromi I, Gomperts R, Martin RL, Fox DJ, Keith TA, Al-Laham MA, Peng CY, Nanayakkara A, Gonzalez C, Challacombe M, Gill PMW, Johnson BG, Chen W, Wong MW, Andres JL, Head-Gordon M, Replogle ES, Pople JA (1998) GAUSSIAN 98. Gaussian, Pittsburgh, Pa
8. (a) Becke AD (1993) J Chem Phys 98: 5648; (b) Lee C, Yang W, Parr RG (1988) Phys Rev B 37: 785
9. Stephens PJ, Devlin FJ, Frisch MJ, Chabalowski CF (1994) J Phys Chem 98: 11623
10. (a) St-Amant A, Salahub DR (1990) Chem Phys Lett 169: 387; (b) Salahub DR, Fournier R, Mylynarski P, Papai I, St-Amant A, Ushio J (1993) In: Labanowski J, Andzelm J (eds) Density functional methods in chemistry. Springer, Berlin Heidelberg New York, pp 77–100; (c) St-Amant A (1991) PhD thesis. Université de Montréal
11. (a) Perdew JP, Wang Y (1986) Phys Rev B 33: 8800; (b) Perdew JP (1986) Phys Rev B 33: 8822; (c) Perdew JP (1986) Phys Rev B 34: 7406
12. Dean RT, Fu S, Stocker R, Davies MJ (1997) Biochem J 324: 1
13. (a) Stubbe J, van der Donk WA (1998) Chem Rev 98: 705; (b) Stubbe J (1989) Annu Rev Biochem 58: 257; (c) Stubbe J (1988) Biochem 27: 3593
14. von Sonntag C (1987) The chemical basis of radiation biology. Taylor and Francis, London
15. Halliwell B, Gutteridge JMC (1999) Free radicals in biology and medicine. Oxford University Press, New York
16. Varadarajan S, Kanski J, Aksenova M, Lauderback C, Butterfield DA (2001) J Am Chem Soc 123: 5625
17. Rauk A, Armstrong DA (2000) J Am Chem Soc 122: 4185
18. (a) Weltner W Jr (1983) Magnetic atoms and molecules. Van Nostrand, New York; (b) Atherton NM (1993) Principles of electron spin resonance. Horwood, UK; (c) Box HC (1977) Radiation effects: ESR and ENDOR analysis. Academic, New York
19. Morton JR (1964) J Am Chem Soc 86: 2325
20. Teslenko VV, Gromovoi YS, Krivenko VG (1975) Mol Phys 30: 425
21. Sanderud A, Sagstuen E (1998) J Phys Chem B 102: 9353
22. (a) Gauld JW, Eriksson LA, Radom L (1997) J Phys Chem A 101: 1352; (b) Engels B, Eriksson LA, Lunell S (1996) Adv Quantum Chem 27: 297
23. (a) Kong, J, Boyd, RJ (1997) J Chem Phys 107: 6270; (b) Kong J, Boyd RJ (1995) J Chem Phys 102: 3674
24. Wetmore SD, Boyd RJ, Eriksson LA (1997) J Chem Phys 106: 7738
25. (a) Wetmore SD, Boyd RJ, Eriksson LA (1998) J Phys Chem B 102: 5369; (b) Wetmore SD, Himo F, Boyd RJ, Eriksson LA (1998) J Phys Chem B 102: 7484; (c) Wetmore SD, Boyd RJ,

Eriksson LA (1998) J Phys Chem B 102: 9332; (d) Wetmore SD, Boyd RJ, Eriksson LA (1998) J Phys Chem B 102: 10602; (e) Wetmore SD, Boyd RJ, Eriksson LA (1998) J Phys Chem B 102: 7674 (f); Wetmore SD, Boyd RJ, Himo F, Eriksson LA (1999) J Phys Chem B 103: 3051
26. Wetmore SD, Eriksson LA, Boyd RJ In: Eriksson LA (ed) (2001) Theoretical biochemistry, processes and properties of biological systems. Elsevier, The Netherlands, pp409p 409
27. Ban F, Gauld JW, Boyd RJ (2000) J Phys Chem A 104: 5080
28. Ban F, Wetmore SD, Boyd RJ (1999) J Phys Chem A 103: 4303
29. Ban F, Gauld JW, Boyd RJ (2000) J Phys Chem A 104: 8583
30. (a) Ding Y, Krogh-Jespersen K (1992) Chem Phys Lett 199: 261; (b) Barone V, Adamo C, Grand A, Subra R (1995) Chem Phys Lett 242: 351
31. Rega N, Cossi M, Barone V (1998) J Am Chem Soc 120: 5723
32. (a) Nelson WH. (1988) J Phys Chem 92: 554; (b) Nelson WH, Nave CR (1981) J Chem Phys 74: 2710
33. Walsh C (2001) Nature 409: 226
34. Hasserodt J (1999) Synlett 12: 2007
35. (a) Stevenson JD, Thomas NR (2000) Nat Prod Rep 17: 535; (b) Thomas NR (1996) Nat Prod Rep 13: 479
36. Koeller KM, Wong C-H (2001) Nature 409: 232; (d) Seoane G (2000) Curr Org Chem 4: 283
37. List B, Lerner RA, Barbas CF III (2000) J Am Chem Soc 122: 2395
38. (a) Gröger H, Vogl EM, Shibasaki M (1998) Chem Eur J 4: 1137; (b) Machajewski TD, Wong C-H (2000) Angew Chem Int Ed Engl 39: 1352
39. Nelson SG (1998) Tetrahedron Asymm 9: 357
40. Gröger H, Wilken J (2001) Angew Chem Int Ed Engl 40: 529
41. Rankin KN, Gauld JW, Boyd RJ (2002) J Phys Chem A 106: 5155
42. Kirby AJ (1996) Angew Chem Int Ed Engl 35: 707
43. Perrin CL, Nielson JB (1997) Annu Rev Phys Chem 48: 511
44. (a) Kang J, Rebek J Jr (1997) Nature 385: 50; (b) Jubian V, Dixon RP, Hamilton AD (1992) J Am Chem Soc 114: 1120; (c) Jubian V, Veronese A, Dixon RP, Hamilton AD (1995) Angew Chem Int Ed Engl 34: 1237; (d) Kang J, Hilmersson G, Santamara J, Rebek J Jr (1998) J Am Chem Soc 120: 3650
45. (a) Melander C, Horne DA (1996) J Org Chem 61: 8344; (b) Huc I, Pieters RJ, Rebek J Jr (1994) J Am Chem Soc 116: 10296
46. Tominaga M, Konishi K, Aida T (1999) J Am Chem Soc 121: 7704
47. Rankin KN, Gauld JW, Boyd RJ (2000) J Am Chem Soc 122: 5384
48. Rankin KN, Gauld JW, Boyd RJ (2001) J Am Chem Soc 123: 2047
49. Malins DC, Polissar NL, Gunselman SJ (1996) Proc Natl Acad Sci USA 93: 2557
50. Ames BN, Shigenaga MK, Hagen TM (1993) Proc Natl Acad Sci USA 90: 7915
51. Loft S, Poulsen HE (1996) J Mol Med 74: 297
52. Totter TR (1980) Proc Natl Acad Sci USA 77: 1763
53. Ohshima H, Bartsch H (1994) Mut Res 305: 253
54. Hsiao K, Chapman P, Nilsen S, Eckman C, Harigaya Y, Younkin S, Yang FS, Cole G (1996) Science 274: 99
55. Selkoe DJ (1994) Annu Rev Cell Biol 10: 373
56. Youdim MBH, Riederer P (1997) Sci Am 276: 52
57. Oleinick NL, Chiu S, Ramakrishnan N, Xue L (1987) Br J Cancer 55: 135
58. Mee LK, Adelstein SJ (1979) Int J Radiat Biol 36: 359
59. Yamamoto O (1976) In: Smith KC (ed) Aging, carcinogenesis, and radiation biology. Plenum, New York, p 165
60. Gajewski E, Dizdaroglu M (1990) Biochemistry 29: 977
61. Ban F, Lundqvist MJ, Boyd RJ, Eriksson LA (2002) J Am Chem Soc 124: 2753
62. Vaupel P, Kallinowski F, Okunieff P (1989) Cancer Res 49: 6449
63. Horsman MR (1998) Int J Radiat Oncol Biol Phys 42: 701
64. Brown JM (1999) Cancer Res 59: 5863
65. Denny WA, Wilson WR (2000) Expert Opin Inv Drug 9: 2889
66. Brown JM, Siim BG (1996) Semin Radiat Oncol 6: 22
67. Brown JM, Wang LH (1998) Anti-Cancer Drug Des 13: 529
68. Brown JM (1993) Br J Cancer Res 67: 1163
69. Daniels JS, Gates KS, Tronche C, Greenberg MW (1998) Chem Res Toxicol 11: 1254
70. Daniels JS, Chatterji T, MacGillivray LR, Gates KS (1998) J Org Chem 63: 10027
71. Hwang J, Greenberg MM, Fuchs T, Gates KS (1999) Biochemistry 38: 14248
72. Daniels JS, Gates KS (1996) J Am Chem Soc 118: 3380
73. Pogozelski WK, Tullius TD (1998) Chem Rev 98: 1089
74. Ban F, Gauld JW, Boyd RJ (2001) J Am Chem Soc 123: 7320
75. (a) Wetmore SD, Boyd RJ, Eriksson LA (2000) Chem Phys Lett 322: 129; (b) Wetmore SD, Boyd RJ, Eriksson LA (2001) Chem Phys Lett 343: 151
76. (a) Cui Q, Karplus M (2002) J Am Chem Soc 124: 3093; (b) Meuwly M, Karplus M (2002) J Chem Phys 116: 2572
77. (a) Szilagi RK, Musaev DG, Morokuma K (2002) Organometallics 21: 55; (b) Liu Z, Torrent M, Morokuma K (2002) Organometallics 21: 1056